Article

Cell Metabolism

The GABA Transaminase, ABAT, Is Essential for Mitochondrial Nucleoside Metabolism

Graphical Abstract

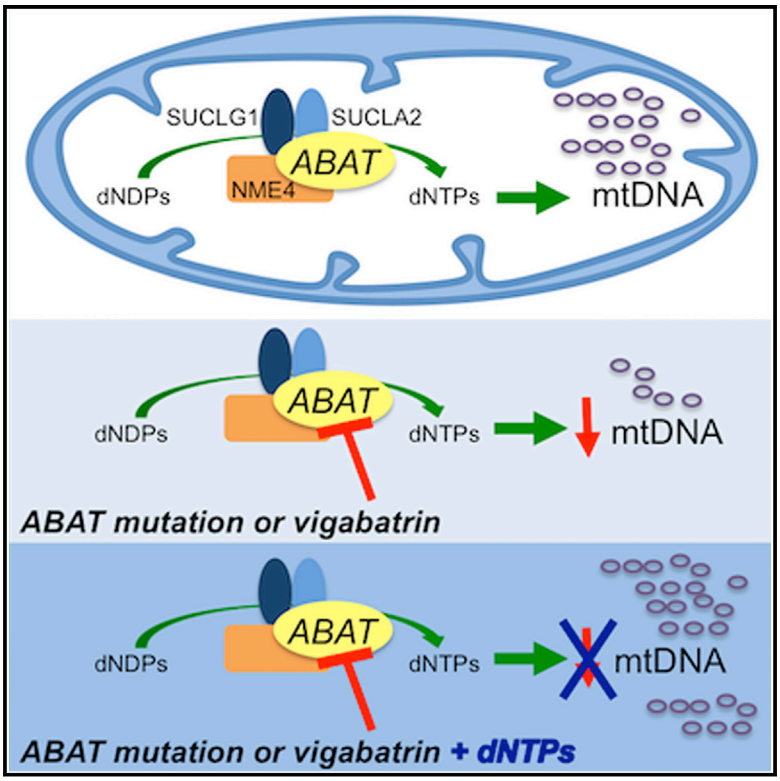

Authors

Arnaud Besse, Ping Wu, ...,
Robert W. Taylor, Penelope E. Bonnen

Correspondence

pbonnen@bcm.edu

In Brief

ABAT is a key enzyme responsible for catabolism of principal inhibitory neurotransmitter γ-aminobutyric acid (GABA). Besse et al. report an essential role for ABAT in a seemingly unrelated pathway, mitochondrial nucleoside salvage, and demonstrate that mutations in this enzyme cause autosomal recessive mtDNA depletion syndrome.

Highlights

- ABAT converts dNDP to dNTP in the mitochondrial nucleoside salvage pathway
- Inhibition of ABAT causes decreased copy number of mitochondrial genome
- mtDNA depletion induced by ABAT inhibition is rescued by dNTP supplementation in vitro
- ABAT causes human mitochondrial DNA depletion syndrome

Besse et al., 2015, Cell Metabolism *21*, 417–427
March 3, 2015
http://dx.doi.org/10.1016/j.cmet.2015.02.008

Cell Metabolism
Article

The GABA Transaminase, ABAT, Is Essential for Mitochondrial Nucleoside Metabolism

Arnaud Besse,[1,2] Ping Wu,[1] Francesco Bruni,[3] Taraka Donti,[1] Brett H. Graham,[1] William J. Craigen,[1] Robert McFarland,[3] Paolo Moretti,[1] Seema Lalani,[1] Kenneth L. Scott,[1] Robert W. Taylor,[3] and Penelope E. Bonnen[1,2,*]
[1]Department of Molecular and Human Genetics
[2]Human Genome Sequencing Center
Baylor College of Medicine, Houston, TX 77030, USA
[3]Wellcome Trust Centre for Mitochondrial Research, Institute of Neuroscience, The Medical School, Newcastle University, Newcastle upon Tyne, NE2 4HH, UK
*Correspondence: pbonnen@bcm.edu
http://dx.doi.org/10.1016/j.cmet.2015.02.008

SUMMARY

ABAT is a key enzyme responsible for catabolism of principal inhibitory neurotransmitter γ-aminobutyric acid (GABA). We report an essential role for ABAT in a seemingly unrelated pathway, mitochondrial nucleoside salvage, and demonstrate that mutations in this enzyme cause an autosomal recessive neurometabolic disorder and mtDNA depletion syndrome (MDS). We describe a family with encephalomyopathic MDS caused by a homozygous missense mutation in *ABAT* that results in elevated GABA in subjects' brains as well as decreased mtDNA levels in subjects' fibroblasts. Nucleoside rescue and co-IP experiments pinpoint that ABAT functions in the mitochondrial nucleoside salvage pathway to facilitate conversion of dNDPs to dNTPs. Pharmacological inhibition of ABAT through the irreversible inhibitor Vigabatrin caused depletion of mtDNA in photoreceptor cells that was prevented through addition of dNTPs in cell culture media. This work reveals ABAT as a connection between GABA metabolism and nucleoside metabolism and defines a neurometabolic disorder that includes MDS.

INTRODUCTION

Mitochondria are essential for maintaining cell physiological processes that include respiration, apoptosis, and calcium buffering. The mitochondrial matrix is the site of multiple metabolic processes including carbohydrate, lipid, amino acid, and nucleoside metabolism. The principal inhibitory neurotransmitter γ-aminobutyric acid (GABA) is catabolized within the mitochondrial matrix by GABA transaminase encoded by 4-aminobutyrate aminotransferase (*ABAT*). Disorders of the GABAergic system can lead to mood and cognitive dysfunction as well as seizures and multiple pharmacological compounds aimed at ameliorating these disorders target this pathway (Millan et al., 2012; Rogawski and Löscher, 2004; Rudolph and Möhler, 2014).

Disturbance of mitochondrial function causes a group of diseases termed primary mitochondrial disorders that can affect every organ system and have a diverse clinical presentation (McFarland et al., 2010). One subtype of primary mitochondrial disorders is caused by a dysfunction in the maintenance of the mitochondrial genome (mtDNA) characterized by a severe loss of mtDNA copy number (Suomalainen and Isohanni, 2010). Clinically, mtDNA depletion syndromes (MDSs) typically present in encephalomyopathic, hepatocerebral, or myopathic forms. MDSs are Mendelian autosomal recessive disorders, and the pathogenic genes responsible play roles in several pathways: replication of the mitochondrial genome (*POLG* [Naviaux and Nguyen, 2004], *PEO1* [Sarzi et al., 2007], and *MGME1* [Kornblum et al., 2013]), mitochondrial nucleoside metabolism (*SUCLG1* [Ostergaard et al., 2007], *SUCLA2* [Elpeleg et al., 2005], *DGUOK* [Mandel et al., 2001], and *TK2* [Saada et al., 2001]), cytosolic nucleoside metabolism (*TYMP* [Nishino et al., 1999] and *RRM2B* [Bourdon et al., 2007]), nucleoside translocator (*SLC25A4* [Palmieri et al., 2005]), and functions yet to be determined (*MPV17* [Spinazzola et al., 2006], and *FBXL4* [Bonnen et al., 2013; Gai et al., 2013]).

Humans with genetic mutations leading to ABAT deficiency are extremely rare (OMIM #613163). Clinical reports describe two families with biochemically confirmed ABAT deficiency (Jaeken et al., 1984; Tsuji et al., 2010). The probands in these families display elevated levels of GABA along with severe psychomotor retardation, intractable seizures, hypotonia, and hyperreflexia. All symptomology was attributed to dysfunction of the GABAergic system.

We report that ABAT provides an essential role in the mitochondrial nucleoside salvage pathway, independent of the GABAergic system, demonstrating that this is a dual-function enzyme. We present a new case of ABAT deficiency whose clinical presentation includes elevated GABA in the brain as well as hallmarks of mitochondrial dysfunction in muscle. We show that genetic and pharmacological inhibition of ABAT in human cells causes a marked loss of mtDNA copy number. Importantly, we also demonstrate that expression of each of the pathogenic *ABAT* mutations reported in humans with elevated levels of GABA leads to pronounced mtDNA depletion, thereby proving the functional consequence of these mutations to be a disturbance of mtDNA maintenance. In addition, we pinpoint precisely where within the mitochondrial nucleoside salvage pathway

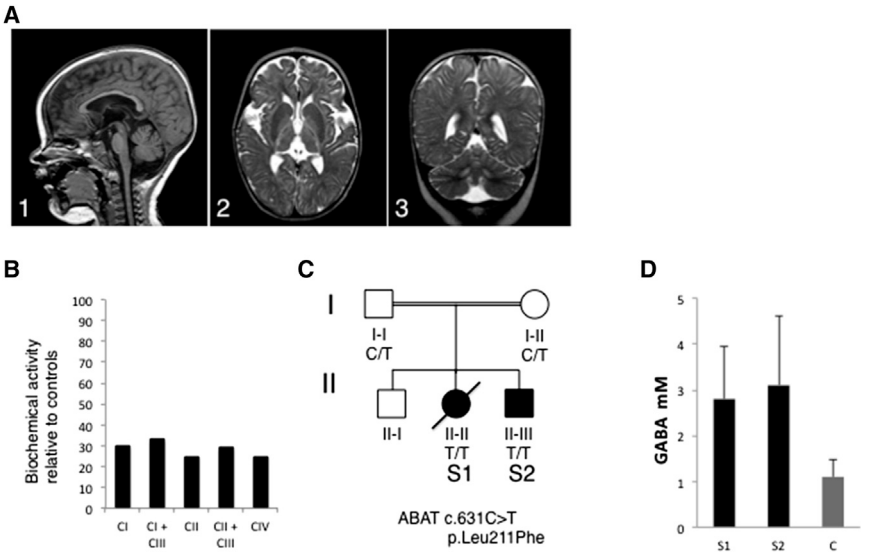

Figure 1. Subjects with *ABAT* Mutations Display Brain Abnormalities and Signatures of Mitochondrial Dysfunction in Muscle

(A) Brain MRI images of S1 at 5 years of age. Image 1 shows a T1-weighted sagittal section demonstrating signs of global cerebral volume loss with thinning of the corpus callosum and atrophy of subcortical structures, brainstem, and cerebellar vermis. Images 2 and 3 show T2-weighted axial and coronal sections demonstrating atrophy and diffuse white matter signal abnormalities in the cerebral hemispheres, prominent atrophy of the thalamus, and noticeable signal abnormalities in the posterior limb of the internal capsule and dentate nuclei.

(B) Biochemical assessment of electron transport chain activity in muscle tissue for S1. Activity is diminished relative to controls across complex I, complexes I + III, complex II, complexes II + III, and complex IV.

(C) Pedigree of Subjects 1 (II-II) and 2 (II-III) shows Mendelian segregation and recessive inheritance of mutation ABAT_NM_000663.3 c.631C>T through the family.

(D) Evaluation of GABA levels in the brain by in vivo proton magnetic resonance spectroscopy is shown in mM units with SD. The amount of GABA in S1 and S2 (black bars) is significantly elevated over age-matched controls (gray bar).

ABAT functions and show that ABAT physically interacts with other proteins known to function in the metabolism of nucleosides within mitochondria. These discoveries illustrate that careful study of individuals with rare diseases can lead to a greater understanding of fundamental biological mechanisms.

RESULTS

Mutations in ABAT Identified in Subjects with Pediatric-Onset Encephalopathy with Neurometabolic and Mitochondrial Dysfunction

Subject 1 (S1) presented at 3 months of age with infantile spasms. Her electroencephalogram (EEG) was characterized by hypsarrhythmia consistent with the diagnosis of West syndrome. MRI of the brain was abnormal, showing symmetric signal abnormalities in several brain regions, including the posterior limbs of the internal capsule, central aspect of the cerebral peduncles, dorsal tegmentum and pons, medulla, and dentate nuclei. She exhibited significant developmental delay when re-evaluated at 5 years of age, with inability to roll over or sit unassisted. This re-evaluation also documented continued seizures despite treatment with anti-epileptic drugs (AEDs) and significant hypotonia with hyperreflexia. Repeat MRI of the brain at 5 years of age showed progressive brain atrophy with substantial thalamic atrophy in addition to moderate thinning of both the corpus callosum and brainstem (Figure 1A) and ophthalmological exam was indicative of cortical visual impairment.

Muscle biopsy was performed to investigate a possible mitochondrial disorder, revealing mild variation of fiber size with rare, large mitochondria of irregular shape; oxidative enzyme reactions including NADH-TR, SDH, and cytochrome *c* oxidase (COX) were reported as normal (no sequential COX/SDH reaction was performed) with a suggestion of an increase in subsarcolemmal enzyme activities. Electron microscopy suggested increased glycogen and lipid droplets. Respiratory chain studies showed significant deficiencies with complexes I, II III, and IV displaying activities of less than 35% of control (Figure 1B). Citrate synthase activity was found elevated to 240% of control mean (controls 9.57 ± 4.72).

Subject 2 (S2) is the younger brother of S1. He followed a highly similar course and clinical presentation as his sister, with psychomotor retardation, intractable seizures, and hypotonia. He had an abnormal EEG that showed generalized cortical dysfunction and multifocal cortical irritability, especially from the right posterior region. At last reporting, age 5 years, he received no benefit from treatment with AEDs. His first MRI at age 1.5 years showed generalized atrophy of the right cerebral hemisphere in addition to signal abnormalities involving bilateral internal capsules and dentate nuclei. Ophthalmological examination showed cortical visual impairment.

Exome sequencing of S1 revealed a homozygous missense variant in *ABAT*. The variant (ABAT NM_000663.3 c.631C > T; NP_000654.2 p.Leu211Phe) was not observed in the ExAC cohort comprised of 61,486 individuals, which includes 5,804 individuals who are attributed as "American" ethnicity. Bioinformatic analyses revealed strong support for pathogenicity of this variant with SIFT and PolyPhen2 giving maximum or "most damaging" scores (SIFT = 0, PolyPhen2 = 1). This nucleotide position also appears highly evolutionarily conserved with GERP score of 5.61 and PhyloP score of 2.66 (Table 1). S2 was shown by Sanger sequencing to be homozygous for the ABAT variant and recessive inheritance was demonstrated with both parents being heterozygous carriers (Figure 1C). Levels of ABAT mRNA and protein in fibroblasts from S1 and S2 were similar to control (Figure S1).

Table 1. In Silico Analysis of *ABAT* Mutations Identified in Subjects with Intractable Seizures, Severe Psychomotor Retardation, and Confirmed Elevated Levels of GABA in the Brain

Gene	Subject	Genome	cDNA	Protein	SIFT	PolyPhen2	GERP++	PhyloP	ExAC_AC
ABAT	S1, S2	16:8862077_C/T	c.631C>T	p.Leu211Phe	0.00	1.00	5.61	2.66	0
ABAT	S3	16:8862105_G/A	c.659G>A	p.Arg220Lys	0.01	0.92	5.61	2.66	0
ABAT	S3	16:8875217_T/C	c.1433T>C	p.Leu478Pro	0.00	1.00	5.39	2.04	0
ABAT	S4	16:8844355_G/A	c.275G>A	p.Arg92Gln	0.60	1.00	5.93	2.80	0
ABAT	S4	16:8844279-?_8844396+?del	c.199-?_316+?del	p.Asn67ValfsTer8	–	–	–	–	0

Mutation nomenclature references human genome build HG19, ABAT NM_000663.4 for cDNA and ABAT NP_000654.2 for protein. Subject S4 has a deletion the removes the fourth coding exon which is approximately 100 base pairs in length, however the boundaries of this mutation are not defined. ExAC_AC = ExAC cohort Allele Count. These mutations were all deposited into ClinVar.

ABAT, also known as GABA-transaminase (GABA-T), catabolizes the neurotransmitter GABA into succinic semialdehyde. Subjects 1 and 2 show excess GABA in the brain by in vivo proton magnetic resonance spectroscopy, supporting the notion that the identified missense variant perturbs function of the ABAT protein. GABA concentrations in the basal ganglia of S1 (2.9 mmol/l) and S2 (3.1 mmol/l) were markedly higher compared to normal mean values for this age range of 1.1 mmol/l ± 0.3 (Figure 1D). The catabolism of GABA through the GABA shunt is known to take place in the mitochondrial matrix, and cellular localization studies confirmed the specific sub-mitochondrial localization of *ABAT* to be the matrix compartment (Figure S2). Subjects from two unrelated families have been clinically described in the literature as having ABAT deficiency (Jaeken et al., 1984; Tsuji et al., 2010). These children showed highly similar clinical presentation to our subjects with severe psychomotor retardation, intractable seizures, hypotonia, and hyperreflexia. However, none of the individuals previously reported as having *ABAT* deficiency were noted to have mitochondrial dysfunction, and no testing of mitochondrial biochemical function was reported. We therefore explored the nature of the mitochondrial deficiency observed in S1 and S2 and tested if the previously reported pathogenic *ABAT* alleles led to mitochondrial dysfunction.

Knockdown of ABAT in Healthy Fibroblasts Causes mtDNA Depletion and Diminished Mitochondrial Membrane Potential

Two independent shRNA hairpins designed to target the 3′ UTR of *ABAT* both resulted in a 50% reduction of mRNA transcript ($p < 0.001$) and protein levels (Figures 2A and 2B) compared to non-targeting (NT) control when virally delivered to normal control fibroblasts. Moreover, this forced reduction of *ABAT* expression by each hairpin led to a concomitant ~50% decrease in both mtDNA copy number ($p < 0.001$) and in the membrane potential ($p < 0.001$) compared to NT controls (Figures 2C and 2D), indicating ABAT is required to maintain these vital features of mitochondrial integrity and function.

All ABAT Mutations Reported to Cause Elevated Levels of GABA Cause mtDNA Depletion in Fibroblasts

The family reported here is the third family documented to have *ABAT* deficiency with confirmed elevated levels of GABA in the brain and a molecular diagnosis (Tsuji et al., 2010). Previously reported probands (S3 and S4) were shown to have compound heterozygous variants in *ABAT* (Figure 3A; Table1). Bioinformatic analyses of these four alleles plus the homozygous variant identified in this study are shown in Table 1. All variants found in *ABAT* deficient subjects are apparently private and were not identified in the ExAC cohort. Additionally, all missense variants received scores for being highly evolutionarily constrained by GERP and PhyloP. Software prediction for the potential of missense variants to disturb protein function assigned two of these variants maximally "damaging" scores by both PolyPhen2 and SIFT. One variant received moderately damaging scores, and one received the maximum score from PolyPhen2 but a "tolerated" score from SIFT. The variant with conflicting results from PolyPhen2 and SIFT received the most highly constrained/conserved scores by GERP++ and PhyloP.

In order to test the functionality of specific genetic alleles, we constructed a novel lentiviral vector (pGIPZ-GW) that, when delivered to cells, permits simultaneous expression of an individual shRNA hairpin and an open reading frame (ORF) (i.e., cDNA) recombined into the Gateway (Invitrogen) ORF acceptor site (Figure 3B). This vector enables knockdown of the endogenous wild-type copy of a gene while expressing a mutant version of the same gene. This allows testing of pathogenic genetic alleles in healthy control cells, alleviating the need for tissue collected from subjects, and provides testing of those alleles in a "healthy" genomic context. In this case, we designed shRNA hairpins to the 3′ UTR of *ABAT* (Figures 2A and 2B) and delivered wild-type (control) or mutant *ABAT* alleles (Figure 3A) into healthy fibroblasts. Importantly, all *ABAT* expression constructs lacked 3′ UTR sequence making them resistant to shRNA-mediated knockdown when delivered with shRNA that targets the 3′ UTR of *ABAT* (Figure 3B). The functionality of each variant was tested by stable transduction of fibroblasts and subsequent quantitation of mtDNA copy number. Cells infected with pGIPZ-GW virus carrying NT shRNA and mCherry (#1) exhibited normal levels of mtDNA as did cells expressing NT shRNA and an ORF encoding wild-type *ABAT* (#3). Cells expressing *ABAT*-specific shRNA and mCherry (#2) (Figure 3C) showed the same level of knockdown of mtDNA as when the *ABAT*-specific shRNA is expressed alone (50%) (Figure 2C). Co-delivery of RNAi-resistant *ABAT* rescued the mtDNA depletion phenotype resulting from *ABAT* shRNA (#4), allowing us to use this system to examine the efficacy of each variant the context of wild-type *ABAT* depletion. Consistent with their proposed roles as pathogenic variants, cells infected with pGIPZ-GW virus carrying each *ABAT* mutation in the presence of ABAT shRNA (#5–#10) exhibit mtDNA copy number

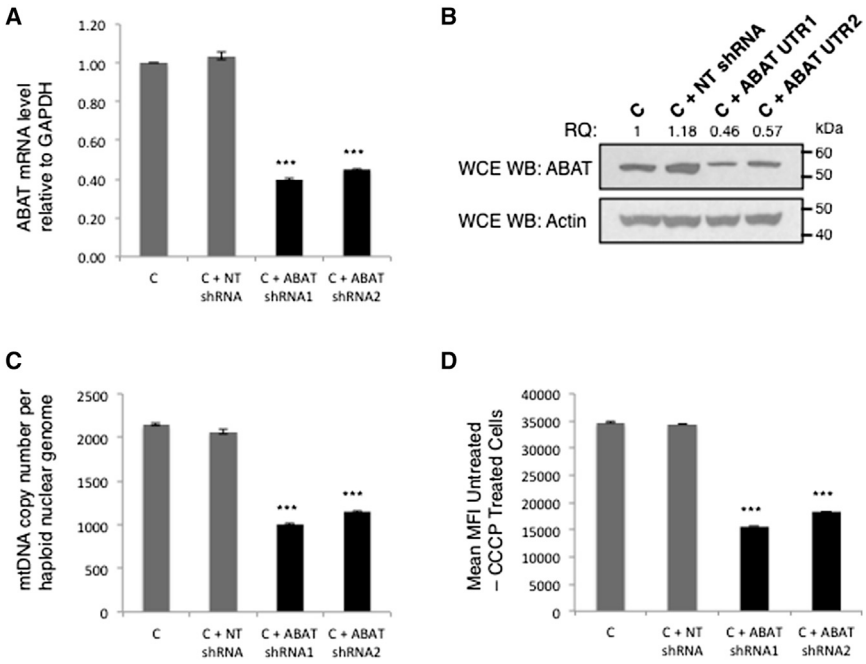

Figure 2. shRNA Knockdown of *ABAT* in Healthy Fibroblasts Results in mtDNA Depletion and Diminished Mitochondrial Membrane Potential

(A and B) Control fibroblasts transfected with two independent shRNAs targeting *ABAT* show *ABAT* transcript levels that are roughly half of *ABAT* transcript levels in controls (A), and western blotting shows ABAT protein levels in these cells are also diminshed by half (B).

(C and D) Likewise, fibroblasts with ABAT mRNA and protein knockdown exhibit significantly diminshed copy number of mtDNA (C) and membrane potential (D) while NT shRNA shows no difference compared to untreated control. In all panels, C is control, C + NT shRNA is control cells transfected with NT shRNA, and C + ABAT shRNA is controls cells transfected with shRNA targeting the 3′ UTR of *ABAT*. *** indicates p value $< 1 \times 10^{-5}$. Error bars indicate SD.

similar to where the *ABAT* shRNA is expressed alone (#2), thus demonstrating the inability of the alleles identified in ABAT deficient subjects to "rescue" the decreased mtDNA copy number induced by knocking down the wild-type copy of *ABAT* present in healthy cells. This confirms that each individual *ABAT* variant found in subjects perturb gene function at the level of being able to properly maintain copy number of the mitochondrial genome.

Non-Proliferating Subject Fibroblasts Demonstrate Low mtDNA Copy Number and Diminished Membrane Potential, and Delivery of Wild-Type ABAT Corrects This Mitochondrial Dysfunction

Each currently described human disease gene causing MDS is shown in Figure 5A along with an illustration of the basic role the protein product plays within the mitochondria. ABAT localizes to the mitochondrial matrix where other proteins whose disruption leads to mtDNA depletion function in either the mitochondrial nucleoside salvage pathway or mtDNA replication (Figures 5A and S2). We hypothesized that in addition to and distinct from its recognized function catabolizing GABA, ABAT may also play a role in one of these mitochondrial processes. dNTPs generated in the cytosol through de novo synthesis or salvage are utilized by the mitochondria for mtDNA maintenance. However, these pathways are coordinated with the cell cycle. When cells are in G0, nuclear DNA replication is halted and cytosolic nucleoside pathways are downregulated, but mitochondria continue to replicate (Pica-Mattoccia and Attardi, 1972). Consequently, in quiescent or post-mitotic cells, mitochondria are forced to rely on the mitochondrial nucleoside salvage pathway to deliver nucleotides to the replication machinery of the mitochondrial genome. In order to test our hypothesis that ABAT participates in either mtDNA replication or nucleoside salvage pathways, we devised a series of experiments aimed at differentiating these two functions in both healthy and ABAT-deficient subject cells.

mtDNA copy number was determined in subject fibroblasts while grown in normal medium (cycling cells) versus low serum medium (LSM) (quiescent cells). Fibroblasts from subjects with *ABAT* mutation (S1 and S2) have lower mtDNA copy number than controls when grown in normal media (NM) (S1 69%, S2 82%) and decreases when cells are grown in LSM (S1 44% of mean control; S2 55% of mean control) (Figure 4A). Likewise, their mitochondrial membrane potential is lower than control when fibroblasts are cycling (S1 and S2 p value $< 1 \times 10^{-3}$) and becomes more compromised when cells are quiescent (S1 and S2 $p < 1 \times 10^{-5}$) (Figure 4B). In order to determine whether *ABAT* could rescue the mtDNA copy number and membrane potential deficiencies exhibited by S1- and S2-derived fibroblasts, we performed gene rescue studies by stably transducing these cells with either wild-type *ABAT* or vector control (GFP). As shown in Figures 4C and 4D, delivery of wild-type *ABAT* corrects for mtDNA copy number deficiency confirming that the ABAT protein plays a role in this dysfunction (S1 and S2 $p < 1 \times 10^{-5}$).

ABAT Functions in Mitochondrial Nucleoside Salvage Pathway in the Conversion of dNDP to dNTP

The relative levels of mtDNA copy number loss in subject cells whether cycling or quiescent are above the commonly accepted diagnostic threshold for being reported as abnormal ($\leq$30% of control); however, the fact that mtDNA copy number decreases in quiescent cells supports the possibility that ABAT participates in mitochondrial nucleoside salvage. To examine this possibility, a series of "nucleoside rescue" experiments were conducted to pinpoint if and where ABAT plays a role in the mitochondrial nucleoside salvage pathway. Fibroblast cell lines from the two affected siblings S1 and S2 were cultured in LSM with various nucleotide pools: dATP+dGTP, dCTP+dTTP, dADP+dGDP, dCDP+dTDP, dAMP+dGMP, or dCMP+dTMP. As controls, we utilized cells from healthy individuals as well as those derived from children who have MDS caused by pathogenic mutations

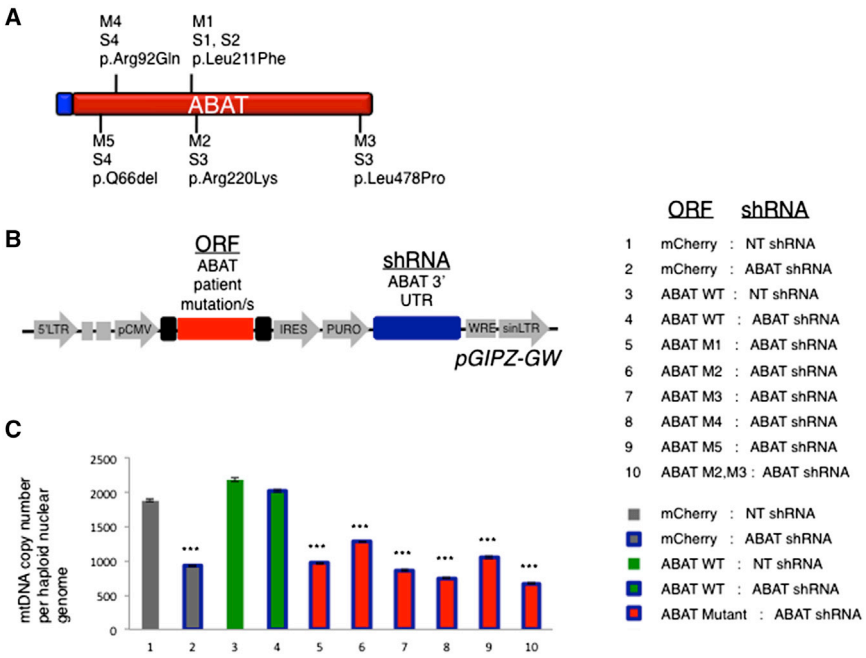

Figure 3. Pathogenic *ABAT* Mutations Identified in Subjects with Elevated GABA Levels Cause a Quantitative Loss of mtDNA Copy Number

(A) Three unrelated families have been identified with *ABAT* deficiency that have a molecular diagnosis and elevated levels of GABA in brain confirmed by MRS. S1 and S2 were affected siblings homozygous for p.Leu211Phe (M1). S3 was compound heterozygous for missense mutations M2 and M3. S4 was compound heterozygous for missense mutation M4 and deletion M5. *ABAT* subject mutations are distributed throughout the length of the protein.

(B) A first-in-kind lentiviral vector was created to simultaneously deliver an shRNA and an ORF by modifying the pGIPZ expression vector.

(C) Healthy cells were transduced with constructs containing shRNA targeted to *ABAT* 3′ UTR and ORFs containing each subject mutation. All mutations resulted in decreased mtDNA copy number. *** indicates p value < 1×10^{-5}. Error bars indicate SD.

in *SUCLA2* (homozygous NP_003841.1: p.Gly424Aspfs*18) and *DGUOK* (homozygous NP_550438.1 p.Phe256*) (Al-Hussaini et al., 2014), genes known to participate in the conversion of dNDP to dNTP and the phosphorylation of purine deoxynucleosides in the mitochondria, respectively. Mouse embryonic fibroblasts (MEFs) derived from a *SUCLA2*$^{-/-}$ gene trap mouse (Donti et al., 2014) were also tested. Healthy cells showed the same level of mtDNA copy number when grown in all conditions (Figure 5B). Cells from S1, S2, *SUCLA2* subject, and *SUCLA2*$^{-/-}$ MEFs show the same pattern of response to exposure to nucleosides: full rescue of mtDNA copy number when grown in the presence of dNTPs and depletion of mtDNA under all other growth conditions (Figure 5B). The DGUOK subject cells show normal levels of mtDNA only when grown in the presence of deoxypurines. This rescue of mtDNA copy number was also successful in cells infected with ABAT-specific shRNA (Figure 5C), imparting additional support that providing cells with dNTPs rescues the genetic inhibition of ABAT with regard to mtDNA genome maintenance. This highlights that ABAT, like SUCLA2, plays a role in the production of dNTPs in the mitochondria.

We further explored this possibility by testing if ABAT binds to other proteins known to function at this step of the mitochondrial nucleoside salvage pathway, namely SUCLG1, SUCLG2, SUCLA2, and NME4. Succinyl-CoA Synthase (SCS) is a Kreb's cycle enzyme that reversibly catalyzes the synthesis of succinyl-CoA. SCS is a heterodimer of SUCLG1 and either SUCLG2 or SUCLA2. Children with MDS have been reported with *SUCLG1* and *SUCLA2* mutations. While no patients have been reported with *SUCLG2* mutations, knockdown of *SUCLG2* in fibroblasts results in decreased mtDNA content (Miller et al., 2011). NME4 is a mitochondrial nucleoside diphosphate kinase (NDPK), a family of proteins known to catalyze the exchange of γ-phosphate between di- and tri-phosphonucleosides that has been shown to associate with SCS (Kowluru et al., 2002; Tokarska-Schlattner et al., 2008). Co-immunoprecipitation studies show that ABAT physically interacts with SUCLG1, SUCLG2, SUCLA2, and NME4 (Figures 5D and 5E). Additionally, we show that NME4 also binds SUCLG1, SUCLG2, and SUCLA2 (Figures 5F and 5G–5K). These experiments also confirm that SUCLG1 and SUCLG2 bind each other while SUCLA2 binds SUCLG1 but not SUCLG2 (Figures 5F and 5G–5I).

Pharmacological Inhibition of ABAT with Vigabatrin Causes mtDNA Depletion in Photoreceptor Cells, which Is Rescued by dNTP Media Supplementation

Vigabatrin is an irreversible inhibitor of ABAT that is indicated for treatment of epilepsy. It is typically reserved for patients who do not respond to other drugs, because up to 40% of individuals who receive vigabatrin treatment suffer retinopathy resulting in visual field defects (Wild et al., 2007). Despite being non-responsive to other AEDs, neither subject in this study was ever treated with vigabatrin. We tested if pharmacological inhibition of ABAT by vigabatrin causes depletion of mtDNA in murine retinal cells. Cells were placed in G0 through growth in LSM and cultured for 10 days with vigabatrin at doses analogous to those given to humans, as indicated by serum concentration. The level of mtDNA in cells showed a dose-dependent response to vigabatrin, with an already significant drop in mtDNA at 100 μM dose, half the normal copy number of mtDNA at 200 μM, and one-third normal copy number at 300 μM (Figure 6A). Culturing cells under the same conditions but with the addition of dNTPs to the media completely prevents any depletion of mtDNA (Figure 6B).

DISCUSSION

This work demonstrates that ABAT plays an essential role in the conversion of dNDPs to dNTPs in the mitochondrial nucleoside

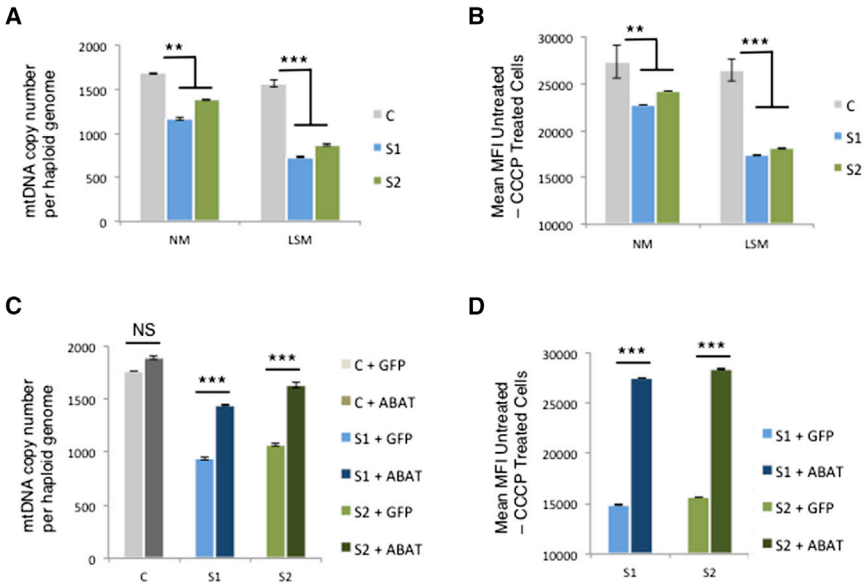

Figure 4. G0 Fibroblasts from Subjects with *ABAT* Mutations Show Deficits in mtDNA Copy Number and Mitochondrial Membrane Potential and Transduction with Wild-Type *ABAT* cDNA Rescues Cellular Dysfunction

Fibroblasts grown in LSM enter the G0 phase of the cell cycle and become quiescent.

(A) Subjects with *ABAT* mutation have lower mtDNA copy number than controls when grown in normal media (NM), and their mtDNA copy number decreases to roughly half that of healthy controls when grown in LSM.

(B) Mitochondrial membrane potential is diminished compared to controls when subject cells are cycling and in G0.

(C and D) Subject cells transduced with wild-type *ABAT* ORF (ABAT-WT) show significantly increased mtDNA copy number (C) and membrane potential (D) when compared to subject cells transduced with GFP. Fibroblasts were allowed to recover from lentiviral infection and then grown in LSM for 7 days prior to harvesting for quantitation of mtDNA. ** indicates p value < 1×10^{-3}. *** indicates p value < 1×10^{-5}. Error bars indicate SD.

salvage pathway and causes a neurometabolic disorder that includes encephalomyopathic MDS. We present a new family with ABAT deficiency and show the affected subjects have elevated GABA in the brain as well as hallmarks of mitochondrial dysfunction in muscle. Furthermore, we show that all *ABAT* mutations reported in humans with elevated levels of GABA lead to a marked mtDNA depletion in vitro. Additionally, inhibition of *ABAT* through mutation, shRNA knockdown, or the drug vigabatrin causes loss of quantitative mtDNA copy number that is rescued by the supplementation of dNTPs.

We show that ABAT binds each of the three protein components of SCS (SUCLG1, SUCLG2, and SUCLA2) as well as the NDPK NME4. SCS serves as a precedent for dual-function enzymes that play a metabolic role in the mitochondrial matrix and in the maintenance of mtDNA. SCS reversibly catalyzes the synthesis of succinyl-CoA and on generation of succinate converts GDP to GTP. Individuals with MDS can have mutations in *SUCLG1* and *SUCLA2*, but the precise role of SCS in mtDNA maintenance remains unknown. Previous studies have indicated an affiliation between SCS and the mitochondrial NDPK NME4 (Kowluru et al., 2002), and in this report we demonstrate specific binding between the individual protein components of SCS and NME4. NME4 is the only mammalian NDPK with a mitochondrial targeting leader sequence and confirmed mitochondrial localization (Tokarska-Schlattner et al., 2008), but its precise function(s) within the mitochondria remains undetermined. While NDPKs exhibit a lack of substrate specificity and can produce nucleoside triphosphates from all canonical nucleoside diphosphates (Lacombe et al., 2000), they typically utilize the phosphate from ATP to generate dNTPs, in particular dGTP. This confirmation of physical interaction between SCS and NME4 supports the possible role these two enzymes play in homeostasis of GDP/GTP and mitochondrial iron metabolism (Bishop et al., 2012; Gordon et al., 2006) as well as the maintenance of mitochondrial nucleoside pools.

Nucleoside rescue studies strongly support the hypothesis that ABAT and SCS play a role in the conversion of dNDPs to dNTPs. We recapitulate the results of previous studies in cellular models of DGUOK where media supplementation with dAMP and dGMP elevates mtDNA copy number to control levels (Saada, 2008; Taanman et al., 2003). In this study, DGUOK serves as a control and validates our experimental approach. Supplementation of either dA/GTP or dC/TTP but not dNDPs rescues mtDNA copy number in multiple cellular models of ABAT and SUCLA2 deficiency. These nucleoside rescue studies alongside the confirmed protein interactions highlight a role for these two proteins in the generation of dNTPs from dNDPs. Further work is required to delineate the precise roles that ABAT, SUCLG1, SUCLG2, and SUCLA2 each play in this process. Similar to the findings in cellular models of TYMP deficiency indicating that an insufficiency of one or more nucleosides rather than an imbalance of nucleosides pools may be the fundamental cause of depletion of mtDNA in TYMP deficiency (González-Vioque et al., 2011), these ABAT, SUCLA2, and DGUOK nucleoside rescue studies also lend support for the idea that a lack of dNTPs available to the mitochondrial replication machinery causes mtDNA depletion, although more work is needed to dissect the precise cause of mitochondrial toxicity in vivo.

Individuals with MDS due to mutations in *SUCLG1* and *SUCLA2* show some phenotypic overlap with subjects with *ABAT* deficiency. *SUCLG1-SUCLA2* MDS is of the encephalomyopathic form and manifests with clinical features that include severe hypotonia, dystonia, developmental delay, sensorineural hearing loss, and lactic acidosis. In contrast to *SUCLA2* and *SUCLG1* patients, urine organic acids and lactate were normal in *ABAT* subjects. Cultured skin fibroblasts from patients with MDS due to *ABAT*, *SUCLA2*, *SUCLG1*, or *DGUOK* all show levels of mtDNA within the diagnostic "normal" range when grown in standard culture conditions. Likewise, measurements of electron transport chain biochemical activity in patient fibroblasts and

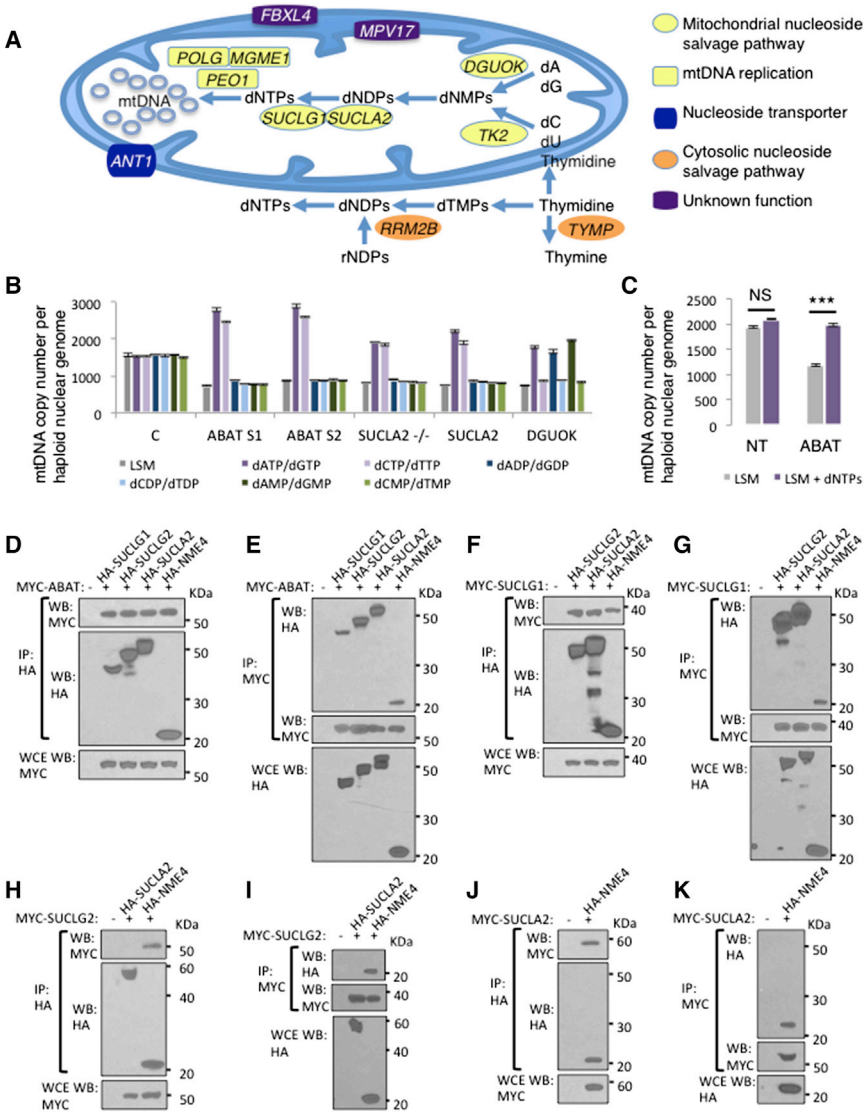

Figure 5. ABAT Functions in the Conversion of dNDP to dNTP in the Mitochondrial Nucleoside Salvage Pathway

(A) Genes known to cause human MDSs are shown with their function indicated as known.

(B and C) (B) Fibroblasts from two subjects with *ABAT* mutations (S1 and S2) were tested in parallel with fibroblasts from individuals with MDS due to *SUCLA2* mutation (homozygous p.Gly424Aspfs*18), *DGUOK* mutation (homozygous p.Phe256*), MEF from *SUCLA2*$^{-/-}$ gene trap mouse, and healthy control (C). Fibroblasts were synchronized in G0 by growth in LSM and then nucleosides (dNTP, dNDP, or dNMP) were added to replica-plated cells. *ABAT* and *SUCLA2* mutant cells show the same level of mtDNA depletion in LSM (50% of control) and same response to media nucleoside supplementation: rescue of mtDNA depletion when either dATP/dGTP or dCTP/dTTP are added to media.

(C) Fibroblasts transduced with ABAT shRNA show 50% mtDNA copy number compared to control, and this is restored to 100% of control with media supplementation with dNTPs.

(D and E) SUCLG1, SUCLG2, SUCLA2, and NME4 participate in the conversion of dNDP to dNTP in mitochondria. Co-IP experiments show that ABAT binds all four of these proteins.

(F–K) Additionally, each possible pairwise binding between SUCLG1, SUCLG2, SUCLA2, and NME4 was tested. SUCLG1 binds SUCLG2, SUCLA2, and NME4. SUCLG2 binds NME4 but not SUCLA2. SUCLA2 also binds NME4. *** indicates p value $< 1 \times 10^{-5}$. Error bars indicate SD.

in healthy fibroblasts transduced with shRNA targeting ABAT show some appreciable deficiencies, but none outside the diagnostic normal range (Figure S4). Once cells are induced into quiescence through growth in LSM, patient fibroblasts harboring *ABAT*, *SUCLA2*, and *DGUOK* mutations show marked mtDNA depletion with 50% of normal copy number (*SUCLG1* patient cells were not available for testing). Hence, in fibroblasts from MDS subjects with mutations in genes involved in mitochondrial nucleoside metabolism, the mtDNA copy number is not sufficiently low to be classed as ''definitively defective'' within a diagnostic setting, but a significant decrease is observed between cycling and quiescent cells. This is consistent with ABAT, SCS, and DGUOK being essential for the mitochondrial nucleoside salvage pathway, which is primarily utilized during G0 when cytosolic nucleoside salvage pathways are downregulated.

The most common human inborn error of metabolism in the GABA degradation pathway is succinic semialdehyde dehydrogenase deficiency (SSADHD) (OMIM #271980), an autosomal recessive disorder characterized by mutations in *ALDH5A1* leading to the elevation of γ-hydroxybutyric acid (GHB) and GABA (Chambliss et al., 1998). Clinical presentation of SSADHD overlaps with ABAT deficiency and includes developmental delay, hypotonia, hyporeflexia, ataxia, and seizures (Knerr et al., 2007). Individuals with *ABAT* mutations may appear similar to more severe cases of SSADHD, and it is important to note these two disorders can be distinguished through measurement of GHB, which is not elevated in ABAT deficiency.

Our findings reveal ABAT to be an enzyme of dual function, its deficiency leading to a neurometabolic disorder as well as a loss of mtDNA copy number. Given the phenotypic overlap between neurometabolic disorders and primary mitochondrial disorders, it is difficult to ascribe which pathological process, depletion of ATP or disrupted GABA metabolism, is largely responsible for the clinical and diagnostic observations. For example, measurement of respiratory chain biochemical activities in muscle showed multiple respiratory chain complex abnormalities, including loss of complex II activity. This enzyme is encoded solely by nuclear genes, and consequently, a decrease in mtDNA copy number would not be expected to affect this activity. The fact that complex II activity is decreased in subjects with *ABAT* mutation suggests factors outside of decreased mtDNA copy number contribute to OXPHOS dysfunction in muscle, but it

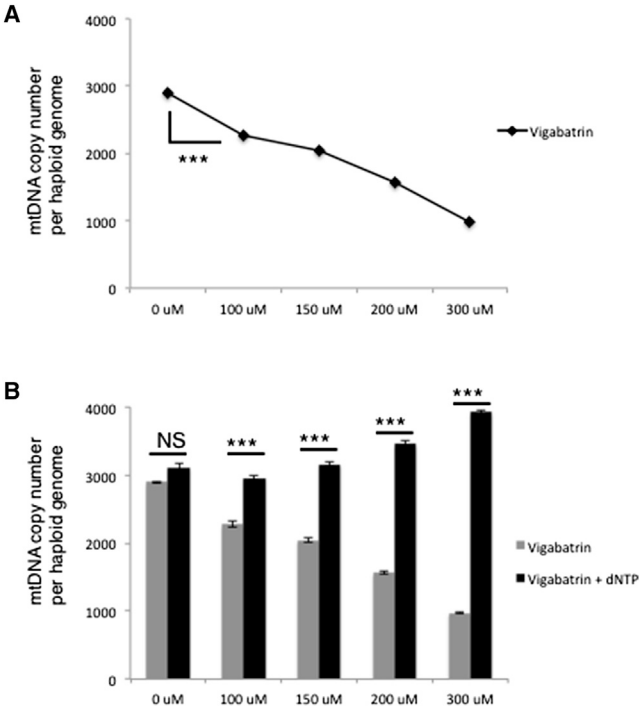

Figure 6. Pharmacological Inhibition of ABAT with Vigabatrin Causes mtDNA Depletion in Photoreceptor Cells That Is Rescued by Media Supplementation with dNTPs

(A and B) (A) Photoreceptor cells were grown in the presence of Vigabatrin in varying doses (0–300 μM) and (B) Vigabatrin plus dNTPs. *** indicates p value < 1×10^{-5}. Error bars indicate SD.

does not necessarily indicate that mtDNA depletion is not contributing to the loss of enzyme activity or that disturbance of GABA catabolism directly causes loss of complex II activity. Nevertheless, our data clearly demonstrate an essential role for ABAT in the conversion of dNDP to dNTP within mitochondria, and as such patients with pathogenic *ABAT* mutations should be classed as having both a neurometabolic disorder and a disorder of mtDNA copy number maintenance. The discovery that ABAT plays an essential role in nucleoside metabolism may reveal insights into the mechanism underlying the retinal defects often observed in individuals receiving vigabatrin treatment. In cellular models, we observed half the normal copy number of mtDNA at 200 μM dose of vigabatrin (Figure 6), which falls within the serum levels corresponding to the dosage range administered to adults (Lindberger et al., 2003). This same reduction of mtDNA copy number is seen in fibroblasts from subjects with ABAT mutations, as well as individuals with mutations in *SUCLA2* or *DGUOK* and MEFs from *SUCLA2*$^{-/-}$ mouse (Figures 4 and 5). Remarkably, this depletion is completely prevented by co-treatment of cells with vigabatrin plus dNTPs. Vigabatrin exposure would be expected to result in undesired effects in tissues that rely most heavily on the mitochondrial nucleoside pathway, like eye and brain. However, additional factors influence the effects of vigabatrin on specific tissues, and consequently, any undesired effects due to loss of mtDNA copy number would not necessarily be expected to be the same across all non-cycling tissues. For example, vigabatrin concentration has been shown in animal models to accumulate 18.5 times higher in retina than brain (Sills et al., 2003). Taken together, this work reveals a potential cause for the visual field defects commonly occurring with vigabatrin treatment and indicates nucleosides as having therapeutic potential to prevent this side effect.

ABAT deficiency causes mtDNA depletion syndrome as well as a neurometabolic disorder of GABA degradation that shares phenotypic overlap with individuals with mutations in *SUCLG1*, *SUCLA2*, and *ALDH5A1*. This work places ABAT in a key role in mitochondrial nucleoside metabolism and identifies SUCLG1, SUCLG2, SUCLA2, and NDPK as protein interactors for ABAT. It will be important to learn if the catabolism of GABA by ABAT is coordinated with the production of dNTPs in the mitochondria and if modulation of dNTP levels accessible to mitochondria can be achieved as a therapeutic for individuals with deficiency in this pathway whether genetically or pharmacologically induced.

EXPERIMENTAL PROCEDURES

Subjects

Subjects 1 and 2 are affected siblings in a family of Mexican origin. The family self-reports distant consanguinity of unspecified relationship. Informed consent was obtained for all subjects approved by local Institutional Review Boards. Genomic DNA was extracted from cultured fibroblasts according to standard protocols.

Proton Magnetic Resonance Spectroscopy

Proton magnetic resonance spectroscopy (^{1}H-MRS) was obtained using a single-voxel stimulated-echo acquisition mode (SV-STEAM) sequence (Frahm et al., 1987) (TE/TR = 20/2,000 ms) on a 3T Philips Achieva (Best, Netherlands). Post-processing was performed using LCModel, version 6.1-4, to quantify the spectra (Provencher, 1993). Region of interest was placed at the level of the basal ganglia: LCModel output of in vivo ^{1}H-MRS region of interest volume, 10–17.5 ml; TE/TR, 20–30/2,000 ms; number of averages 128.

Mitochondrial Respiratory Chain Activity Assays

The activities of individual respiratory chain complexes were measured in skeletal muscle homogenates and cultured fibroblasts as described previously (Kirby et al., 2007). Enzymatic activity is expressed relative to citrate synthase and is shown as a percentage of normal controls.

Identification, Verification, and Annotation of Subject Mutations

S1 was sequenced by whole-exome capture using VCROME capture assay (Bainbridge et al., 2011). Sequence data were aligned, single nucleotide variants (SNVs) and small insertions and deletions (InDels) were called by GATK (DePristo et al., 2011), and quality control filtering of variants was based on coverage, strand bias, mapping quality, and base quality. Custom Perl scripts were used to annotate variants. Several metrics for prediction of potential functional consequences of variants were applied: SIFT (Ng and Henikoff, 2001) and PolyPhen2 (Adzhubei et al., 2010), GERP (Davydov et al., 2010), and PhyloP (A. Siepel et al., 2006, RECOMB, conference). Filtering of variants included five criteria: (1) allele frequency must be less than 1% in any reference population. (2) PhyloP must be greater than two OR GERP greater than five or maximum damaging scores for SIFT or PolyPhen2. (3) Variants should be homozygous or compound heterozygous. (4) Variants must not be present in a segmental duplication. (5) Variant must not be present in a SNP cluster defined as the presence of five or more SNVs within 1 Kb of each other. The Exome Aggregation Consortium (ExAC) Cohort was used as reference population data for variant filtering of exome data and for checking the allele frequency of ABAT variants in found in subjects with ABAT deficiency (Exome Aggregation Consortium Cohort, Cambridge) (http://exac.broadinstitute.org, accessed November, 2014).

The *ABAT* variant identified through exome sequencing in S1 was orthogonally validated, and recessive segregation through the subject's pedigree was confirmed with Sanger sequencing.

All genetic alleles studied were submitted to ClinVar http://www.ncbi.nlm.nih.gov/clinvar/ and were annotated in reference to ABAT NM_000663.4 for cDNA and NP_000654.2 for protein.

Primary Fibroblast Cell Culture

Human and mouse embryonic fibroblasts were grown in MEM (Life Technologies) supplemented with FBS to 10%, 1× MEM-vitamins, 2 mM L-glutamine, 1 mM sodium pyruvate, 1× penicillin/streptomycin, 1× non-essential amino acids, and 0.41 μM uridine.

shRNA Knockdown of ABAT

Oligonucleotides containing shRNA hairpins that target the 3′ UTR of ABAT were custom designed and cloned into the pGIPZ vector (GE Healthcare). Control fibroblasts were infected with two independent shRNA hairpins plus a scrambled shRNA, and 72 hr post-infection QRT-PCR and western blot for ABAT were performed on these cells as described below.

Quantitation of mtDNA Copy Number

Mitochondrial genome copy number was determined by real-time quantitative PCR as described previously (Bonnen et al., 2013). Briefly, the mitochondrial genome copy number is determined relative to the nuclear genome using the *MTND1* region of mitochondrial genome and *B2M* as the nuclear genome normalizer. The assay utilized iTaqTM SYBR Green Supermix with ROX (Bio-Rad Laboratories, Hercules, CA) and was conducted in triplicate on total genomic DNA and shown as the average and SD.

Assessment of Mitochondrial Membrane Potential

Mitochondrial membrane potential was assessed as previously described (Bonnen et al., 2013). Cells were grown to confluence, counted, and then were either stained directly with DilC1(5) or pre-incubated with carbonyl cyanide 3-chlorophenylhydrazone (CCCP) prior to staining (MitoProbe DilC1(5) Assay kit for Flow Cytometry, Life Technologies). Results are reported as the difference between the mean fluorescence intensity (MFI) of cells that received treatment with CCCP versus those that did not. Assays were conducted in triplicate and shown as the average and SD.

Quantitation of ABAT mRNA by qRT-PCR

RNA was extracted and cDNA synthesized using standard protocols. Quantitative real-time PCR experiments were performed using a StepOne Plus RT-PCR system (Applied Biosystems), RT2 qPCR Primer Assays for Human *GAPDH* and *ABAT* (SABiosciences), and PerfeCTa SYBR Green FastMix ROX (Quanta Biosciences). The cycle of threshold value (Ct) was normalized to the transcripts for the housekeeping gene *GAPDH*. All assays were conducted in triplicate and the results are shown as the average and SD.

Vector Construction for pGIPZ-GW

The pGIPZ-GW vector, which allows simultaneous expression of ORF and shRNA, was generated by introducing a Gateway cloning cassette and preceding CMV promoter generated using the Fusion HD Cloning Kit (Clontech) and the vector pLenti6.3 V5/DEST (Life Technologies) as PCR template into the pGIPZ vector restriction digested with XbaI/BsrGI.

Cloning and Functionally Testing ABAT Mutations

Wild-type ABAT entry ORF clone (NM_000663.3; clone ID: IOH13638) was obtained from Invitrogen. ABAT mutant ORFs were constructed by site-directed mutagenesis using the wild-type ORF template and the following mutant PCR primers:

M1(ORF631C > T; L211F):ctgccccgactacagcatcTtctccttcatgggcgcgttccatgggagga;

M2(ORF659G > A; R220K):atgggcgcgttccatgggaAgaccatgggttgcttagcgaccacgcactc;

M3(ORF1433T > C; L478P):attcgtttccgtcccacgcCggtcttcagggatcaccacgctcacctgtt;

M4(ORF 275G > A; R92Q):gttgatgtggacggcaaccAaatgctggatctttattcccagatctcctc).

ORFs were recombined into destination vector (pLex302) with LR recombinase (Invitrogen). Mutation M5 (Q66 del) was generated by PCR using ABAT-specific primers fused to attB1/B2 recombination sequences (Invitrogen) designed following the manufacture's recommendations, followed by recombination of the PCR product into entry vector (pDONR221; Invitrogen) with BP recombinase (Invitrogen) for subsequent delivery to destination vector as specified above.

shRNA hairpins that target the ABAT 3′ UTR and a scrambled shRNA were transferred from the pGIPZ vector into the pGIPZ-GW by enzymatic digestion (XhoI + MluI) and ligation. Then the cDNAs corresponding to mCherry, ABAT wild-type, or ABAT mutants were transferred from Donor223 vector (Invitrogen) into the pGIPZ-GW by LR recombination reaction (Invitrogen).

Virus production was conducted as previously described (Bonnen et al., 2013). Infectious lentiviral supernatant was used to infect healthy growing fibroblasts with polybrene (Sigma) before selection by puromycin.

Gene Rescue

Patient and control fibroblasts were stably infected with a pLX302 lentiviral mammalian expression vector system expressing *EGFP* and *ABAT* cDNA (NM_000663.4) as previously described (Bonnen et al., 2013).

Nucleotide Rescue

Healthy, patient, and mouse embryonic fibroblasts were seeded at a concentration of 50,000 cells per well and grown in DMEM (Thermo Scientific Hyclone) with 15% FBS (Atlanta Biologicals) until reaching confluence. The growth medium was then removed, and the cells were washed three times with 1× PBS. LSM (DMEM with 0.5% FBS) was added and the cells cultured for 24 hr. Subsequently, LSM was replaced with fresh LSM containing either dNMP, dNDP, or dNTP (Sigma-Aldrich) each at a final concentration of 50 μM. Cells were cultured under these conditions for 7 days and then harvested.

Fibroblast cell lines used as controls in this experiment included an individual with MDS due to homozygous *SUCLA2* NP_003841.1: p.Gly424Aspfs*18 mutation and a subject who is homozygous for *DGUOK* NP_550438.1 p.Phe256* (Al-Hussaini et al., 2014) (OMIM #612073 and OMIM #251880). An additional control was mouse embryonic fibroblasts from a *SUCLA2*$^{-/-}$ gene trap mouse (Donti et al., 2014).

Co-Immunoprecipitation and Western Blotting

Proteins of interest (ABAT, SUCLG1, SUCLG2, SUCLA2, and NME4) were tagged with HA and Myc tags by PCR reaction using primers that contained Gateway Cloning attB sites to facilitate insertion of the PCR products into Donor223 vector (Invitrogen). Tagged proteins were next transferred by LR recombination reaction into a mammalian expression vector pLenti6.3/V5-Dest vector (Invitrogen).

HEK293T cells were transfected with tagged proteins using Lipofectamine 2000 (Invitrogen) and harvested 48 hr after transfection. For immunoprecipitation, equivalent amounts of cell lysates were incubated with primary anti-HA rabbit/mouse (Cell Signaling) or anti-Myc rabbit/mouse (Cell Signaling) antibodies for 2 hr. Then, a 50% slurry of protein A/G-sepharose was added and incubated for 1 hr. Whole-cell extracts and immunoprecipitates were resolved on SDS-polyacrylamide gel electrophoresis (SDS-PAGE) and transferred to Immobilon P PVDF membranes (Millipore). Membranes were immunoblotted overnight at 4°C with the indicated antibodies followed by secondary antibody (Santa Cruz Biotechnology) and visualized using Enhanced Chemiluminescence Western Blotting System (GE Healthcare).

Cellular and Sub-Mitochondrial Fractionation for Localization of ABAT

Subcellular fractions were prepared as described previously (Bruni et al., 2013) with few modifications. HEK293 cells were harvested, resuspended in HB (0.6 M Mannitol, 10 mM Tris-HCl [pH 7.4], and 1 mM EGTA), and subjected to standard differential centrifugation, and the post-mitochondrial supernatant (cytosolic fraction) was retained. To obtain sub-mitochondrial fractions, 650 μg of mitochondria were treated with proteinase K (PK), pelleted and resuspended in HB. Mitoplasts were obtained by resuspending PK-treated mitochondria in 10 mM Tris-HCl and treated with PK. To extract the inner mitochondrial membrane (IMM) proteins, PK-treated mitoplasts were pelleted, and the pellet was dissolved in 100 mM Na_2CO_3 and incubated on ice for 30 min. This was centrifuged at 100,000 × *g* for 15 min at 4°C, and the pellet was dissolved in HB. Proteins (40 μg) from whole-cell lysate, cytosolic, and mitochondrial fractions were loaded onto 12% SDS-PAGE gel, transferred

to PVDF membrane, and immunoblotted with primary antibodies to eIF4E (Cell Signaling), AIF (NEB), GDH (custom made), NDUFA9 (Mitosciences), and ABAT (Abcam).

Vigabatrin Studies in Mouse Photoreceptor Cells

Cells from the immortalized murine retinal cone photoreceptor-derived cell line (661W) were seeded at a concentration of 200,000 cells per well and grown in DMEM (Thermo Scientific Hyclone) with 10% FBS (Atlanta Biologicals) until near confluence. The growth medium was then removed, and the cells were washed three times with 1× PBS. LSM (DMEM with 0.5% FBS) was added and the cells were cultured for 24 hr. Next, LSM was replaced with fresh LSM containing 50 μM dNTP (Sigma-Aldrich) and vigabatrin (Sigma-Aldrich) at 100, 150, 200, or 300 μM. Media was replaced every day until day 10, when cells were harvested.

SUPPLEMENTAL INFORMATION

Supplemental Information includes four figures and can be found with this article online at http://dx.doi.org/10.1016/j.cmet.2015.02.008.

AUTHOR CONTRIBUTIONS

P.E.B. participated in study design, drafting of the manuscript, collection, and analyses of data. K.L.S. and R.W.T. participated in drafting the manuscript and collection and analyses of data. A.B. and F.B. conducted experiments and contributed to drafting the manuscript. P.W. and T.D. conducted experiments. B.H.G., W.J.C., R.M., P.M., and S.L. contributed clinical expertise and interpretation. S.L. clinically evaluated the patient and family. All authors approved the final manuscript.

ACKNOWLEDGMENTS

Research reported in this publication was supported by National Institute of Neurological Disorders and Stroke of the National Institutes of Health under award number R01NS083726. This work was also supported by the Texas Norman Hackerman Advanced Research Program (THECB 02006; NHARP proposal number 0049-0041-2009) to P.E.B. R.M. and R.W.T. are funded by a Wellcome Trust Strategic Award (096919/Z/11/Z), the MRC Centre for Neuromuscular Diseases (G0601943), the Lily Foundation, and the UK NHS Highly Specialised "Rare Mitochondrial Disorders of Adults and Children" Service. This project was supported by the Cytometry and Cell Sorting Core at Baylor College of Medicine with funding from the NIH (AI036211, CA125123, and RR024574) and the expert assistance of Joel M. Sederstrom. We thank the family for participating in this study.

Received: October 1, 2014
Revised: December 18, 2014
Accepted: February 6, 2015
Published: March 3, 2015

REFERENCES

Adzhubei, I.A., Schmidt, S., Peshkin, L., Ramensky, V.E., Gerasimova, A., Bork, P., Kondrashov, A.S., and Sunyaev, S.R. (2010). A method and server for predicting damaging missense mutations. Nat. Methods *7*, 248–249.

Al-Hussaini, A., Faqeih, E., El-Hattab, A.W., Alfadhel, M., Asery, A., Alsaleem, B., Bakhsh, E., Ali, A., Alasmari, A., Lone, K., Nahari, A., Eyaid, W., Al Balwi, M., Craig, K., Butterworth, A., He, L., and Taylor, R.W. (2014). Clinical and molecular characteristics of mitochondrial DNA depletion syndrome associated with neonatal cholestasis and liver failure. J. Pediatr. *164*, 553.e2–559.e2.

Bainbridge, M.N., Wang, M., Wu, Y., Newsham, I., Muzny, D.M., Jefferies, J.L., Albert, T.J., Burgess, D.L., and Gibbs, R.A. (2011). Targeted enrichment beyond the consensus coding DNA sequence exome reveals exons with higher variant densities. Genome Biol. *12*, R68.

Bishop, D.F., Tchaikovskii, V., Hoffbrand, A.V., Fraser, M.E., and Margolis, S. (2012). X-linked sideroblastic anemia due to carboxyl-terminal ALAS2 mutations that cause loss of binding to the β-subunit of succinyl-CoA synthetase (SUCLA2). J. Biol. Chem. *287*, 28943–28955.

Bonnen, P.E., Yarham, J.W., Besse, A., Wu, P., Faqeih, E.A., Al-Asmari, A.M., Saleh, M.A., Eyaid, W., Hadeel, A., He, L., et al. (2013). Mutations in FBXL4 cause mitochondrial encephalopathy and a disorder of mitochondrial DNA maintenance. Am. J. Hum. Genet. *93*, 471–481.

Bourdon, A., Minai, L., Serre, V., Jais, J.P., Sarzi, E., Aubert, S., Chrétien, D., de Lonlay, P., Paquis-Flucklinger, V., Arakawa, H., et al. (2007). Mutation of RRM2B, encoding p53-controlled ribonucleotide reductase (p53R2), causes severe mitochondrial DNA depletion. Nat. Genet. *39*, 776–780.

Bruni, F., Gramegna, P., Oliveira, J.M., Lightowlers, R.N., and Chrzanowska-Lightowlers, Z.M. (2013). REXO2 is an oligoribonuclease active in human mitochondria. PLoS ONE *8*, e64670.

Chambliss, K.L., Hinson, D.D., Trettel, F., Malaspina, P., Novelletto, A., Jakobs, C., and Gibson, K.M. (1998). Two exon-skipping mutations as the molecular basis of succinic semialdehyde dehydrogenase deficiency (4-hydroxybutyric aciduria). Am. J. Hum. Genet. *63*, 399–408.

Davydov, E.V., Goode, D.L., Sirota, M., Cooper, G.M., Sidow, A., and Batzoglou, S. (2010). Identifying a high fraction of the human genome to be under selective constraint using GERP++. PLoS Comput. Biol. *6*, e1001025.

DePristo, M.A., Banks, E., Poplin, R., Garimella, K.V., Maguire, J.R., Hartl, C., Philippakis, A.A., del Angel, G., Rivas, M.A., Hanna, M., et al. (2011). A framework for variation discovery and genotyping using next-generation DNA sequencing data. Nat. Genet. *43*, 491–498.

Donti, T.R., Stromberger, C., Ge, M., Eldin, K.W., Craigen, W.J., and Graham, B.H. (2014). Screen for abnormal mitochondrial phenotypes in mouse embryonic stem cells identifies a model for succinyl-CoA ligase deficiency and mtDNA depletion. Dis. Model. Mech. *7*, 271–280.

Elpeleg, O., Miller, C., Hershkovitz, E., Bitner-Glindzicz, M., Bondi-Rubinstein, G., Rahman, S., Pagnamenta, A., Eshhar, S., and Saada, A. (2005). Deficiency of the ADP-forming succinyl-CoA synthase activity is associated with encephalomyopathy and mitochondrial DNA depletion. Am. J. Hum. Genet. *76*, 1081–1086.

Frahm, J., Merboldt, K., and Hanicke, W. (1987). Localized Proton Spectroscopy using stimulated echoes. J. Magn. Reson. *72*, 502–508.

Gai, X., Ghezzi, D., Johnson, M.A., Biagosch, C.A., Shamseldin, H.E., Haack, T.B., Reyes, A., Tsukikawa, M., Sheldon, C.A., Srinivasan, S., et al. (2013). Mutations in FBXL4, encoding a mitochondrial protein, cause early-onset mitochondrial encephalomyopathy. Am. J. Hum. Genet. *93*, 482–495.

González-Vioque, E., Torres-Torronteras, J., Andreu, A.L., and Martí, R. (2011). Limited dCTP availability accounts for mitochondrial DNA depletion in mitochondrial neurogastrointestinal encephalomyopathy (MNGIE). PLoS Genet. *7*, e1002035.

Gordon, D.M., Lyver, E.R., Lesuisse, E., Dancis, A., and Pain, D. (2006). GTP in the mitochondrial matrix plays a crucial role in organellar iron homoeostasis. Biochem. J. *400*, 163–168.

Jaeken, J., Casaer, P., de Cock, P., Corbeel, L., Eeckels, R., Eggermont, E., Schechter, P.J., and Brucher, J.M. (1984). Gamma-aminobutyric acid-transaminase deficiency: a newly recognized inborn error of neurotransmitter metabolism. Neuropediatrics *15*, 165–169.

Kirby, D.M., Thorburn, D.R., Turnbull, D.M., and Taylor, R.W. (2007). Biochemical assays of respiratory chain complex activity. Methods Cell Biol. *80*, 93–119.

Knerr, I., Pearl, P.L., Bottiglieri, T., Snead, O.C., Jakobs, C., and Gibson, K.M. (2007). Therapeutic concepts in succinate semialdehyde dehydrogenase (SSADH; ALDH5a1) deficiency (gamma-hydroxybutyric aciduria). Hypotheses evolved from 25 years of patient evaluation, studies in Aldh5a1-/- mice and characterization of gamma-hydroxybutyric acid pharmacology. J. Inherit. Metab. Dis. *30*, 279–294.

Kornblum, C., Nicholls, T.J., Haack, T.B., Schöler, S., Peeva, V., Danhauser, K., Hallmann, K., Zsurka, G., Rorbach, J., Iuso, A., et al. (2013). Loss-of-function mutations in MGME1 impair mtDNA replication and cause multisystemic mitochondrial disease. Nat. Genet. *45*, 214–219.

Kowluru, A., Tannous, M., and Chen, H.Q. (2002). Localization and characterization of the mitochondrial isoform of the nucleoside diphosphate kinase in the pancreatic beta cell: evidence for its complexation with mitochondrial succinyl-CoA synthetase. Arch. Biochem. Biophys. *398*, 160–169.

Lacombe, M.L., Milon, L., Munier, A., Mehus, J.G., and Lambeth, D.O. (2000). The human Nm23/nucleoside diphosphate kinases. J. Bioenerg. Biomembr. *32*, 247–258.

Lindberger, M., Luhr, O., Johannessen, S.I., Larsson, S., and Tomson, T. (2003). Serum concentrations and effects of gabapentin and vigabatrin: observations from a dose titration study. Ther. Drug Monit. *25*, 457–462.

Mandel, H., Szargel, R., Labay, V., Elpeleg, O., Saada, A., Shalata, A., Anbinder, Y., Berkowitz, D., Hartman, C., Barak, M., et al. (2001). The deoxyguanosine kinase gene is mutated in individuals with depleted hepatocerebral mitochondrial DNA. Nat. Genet. *29*, 337–341.

McFarland, R., Taylor, R.W., and Turnbull, D.M. (2010). A neurological perspective on mitochondrial disease. Lancet Neurol. *9*, 829–840.

Millan, M.J., Agid, Y., Brüne, M., Bullmore, E.T., Carter, C.S., Clayton, N.S., Connor, R., Davis, S., Deakin, B., DeRubeis, R.J., et al. (2012). Cognitive dysfunction in psychiatric disorders: characteristics, causes and the quest for improved therapy. Nat. Rev. Drug Discov. *11*, 141–168.

Miller, C., Wang, L., Ostergaard, E., Dan, P., and Saada, A. (2011). The interplay between SUCLA2, SUCLG2, and mitochondrial DNA depletion. Biochim. Biophys. Acta *1812*, 625–629.

Naviaux, R.K., and Nguyen, K.V. (2004). POLG mutations associated with Alpers' syndrome and mitochondrial DNA depletion. Ann. Neurol. *55*, 706–712.

Ng, P.C., and Henikoff, S. (2001). Predicting deleterious amino acid substitutions. Genome Res. *11*, 863–874.

Nishino, I., Spinazzola, A., and Hirano, M. (1999). Thymidine phosphorylase gene mutations in MNGIE, a human mitochondrial disorder. Science *283*, 689–692.

Ostergaard, E., Christensen, E., Kristensen, E., Mogensen, B., Duno, M., Shoubridge, E.A., and Wibrand, F. (2007). Deficiency of the alpha subunit of succinate-coenzyme A ligase causes fatal infantile lactic acidosis with mitochondrial DNA depletion. Am. J. Hum. Genet. *81*, 383–387.

Palmieri, L., Alberio, S., Pisano, I., Lodi, T., Meznaric-Petrusa, M., Zidar, J., Santoro, A., Scarcia, P., Fontanesi, F., Lamantea, E., et al. (2005). Complete loss-of-function of the heart/muscle-specific adenine nucleotide translocator is associated with mitochondrial myopathy and cardiomyopathy. Hum. Mol. Genet. *14*, 3079–3088.

Pica-Mattoccia, L., and Attardi, G. (1972). Expression of the mitochondrial genome in HeLa cells. IX. Replication of mitochondrial DNA in relationship to cell cycle in HeLa cells. J. Mol. Biol. *64*, 465–484.

Provencher, S.W. (1993). Estimation of metabolite concentrations from localized in vivo proton NMR spectra. Magn. Reson. Med. *30*, 672–679.

Rogawski, M.A., and Löscher, W. (2004). The neurobiology of antiepileptic drugs. Nat. Rev. Neurosci. *5*, 553–564.

Rudolph, U., and Möhler, H. (2014). GABAA receptor subtypes: Therapeutic potential in Down syndrome, affective disorders, schizophrenia, and autism. Annu. Rev. Pharmacol. Toxicol. *54*, 483–507.

Saada, A. (2008). Mitochondrial deoxyribonucleotide pools in deoxyguanosine kinase deficiency. Mol. Genet. Metab. *95*, 169–173.

Saada, A., Shaag, A., Mandel, H., Nevo, Y., Eriksson, S., and Elpeleg, O. (2001). Mutant mitochondrial thymidine kinase in mitochondrial DNA depletion myopathy. Nat. Genet. *29*, 342–344.

Sarzi, E., Goffart, S., Serre, V., Chrétien, D., Slama, A., Munnich, A., Spelbrink, J.N., and Rötig, A. (2007). Twinkle helicase (PEO1) gene mutation causes mitochondrial DNA depletion. Ann. Neurol. *62*, 579–587.

Sills, G.J., Butler, E., Forrest, G., Ratnaraj, N., Patsalos, P.N., and Brodie, M.J. (2003). Vigabatrin, but not gabapentin or topiramate, produces concentration-related effects on enzymes and intermediates of the GABA shunt in rat brain and retina. Epilepsia *44*, 886–892.

Spinazzola, A., Viscomi, C., Fernandez-Vizarra, E., Carrara, F., D'Adamo, P., Calvo, S., Marsano, R.M., Donnini, C., Weiher, H., Strisciuglio, P., et al. (2006). MPV17 encodes an inner mitochondrial membrane protein and is mutated in infantile hepatic mitochondrial DNA depletion. Nat. Genet. *38*, 570–575.

Suomalainen, A., and Isohanni, P. (2010). Mitochondrial DNA depletion syndromes—many genes, common mechanisms. Neuromuscul. Disord. *20*, 429–437.

Taanman, J.W., Muddle, J.R., and Muntau, A.C. (2003). Mitochondrial DNA depletion can be prevented by dGMP and dAMP supplementation in a resting culture of deoxyguanosine kinase-deficient fibroblasts. Hum. Mol. Genet. *12*, 1839–1845.

Tokarska-Schlattner, M., Boissan, M., Munier, A., Borot, C., Mailleau, C., Speer, O., Schlattner, U., and Lacombe, M.L. (2008). The nucleoside diphosphate kinase D (NM23-H4) binds the inner mitochondrial membrane with high affinity to cardiolipin and couples nucleotide transfer with respiration. J. Biol. Chem. *283*, 26198–26207.

Tsuji, M., Aida, N., Obata, T., Tomiyasu, M., Furuya, N., Kurosawa, K., Errami, A., Gibson, K.M., Salomons, G.S., Jakobs, C., and Osaka, H. (2010). A new case of GABA transaminase deficiency facilitated by proton MR spectroscopy. J. Inherit. Metab. Dis. *33*, 85–90.

Wild, J.M., Ahn, H.S., Baulac, M., Bursztyn, J., Chiron, C., Gandolfo, E., Safran, A.B., Schiefer, U., and Perucca, E. (2007). Vigabatrin and epilepsy: lessons learned. Epilepsia *48*, 1318–1327.